

# Automotive Object Detection via Learning Sparse Events by Temporal Dynamics of Spiking Neurons

Hu Zhang<sup>1,2</sup>Luziwei Leng<sup>2\*</sup>Kaiwei Che<sup>2,3</sup>Qinghai Guo<sup>2</sup>Jiangxing Liao<sup>2</sup>Qian Liu<sup>2</sup>Jie Cheng<sup>2</sup>Ran Cheng<sup>1\*</sup>

## Abstract

*Event-based sensors, with their high temporal resolution (1μs) and dynamical range (120dB), have the potential to be deployed in high-speed platforms such as vehicles and drones. However, the highly sparse and fluctuating nature of events poses challenges for conventional object detection techniques based on Artificial Neural Networks (ANNs). In contrast, Spiking Neural Networks (SNNs) are well-suited for representing event-based data due to their inherent temporal dynamics. In particular, we demonstrate that the membrane potential dynamics can modulate network activity upon fluctuating events and strengthen features of sparse input. In addition, the spike-triggered adaptive threshold can stabilize training which further improves network performance. Based on this, we develop an efficient spiking feature pyramid network for event-based object detection. Our proposed SNN outperforms previous SNNs and sophisticated ANNs with attention mechanisms, achieving a mean average precision (map50) of 47.7% on the Gen1 benchmark dataset. This result significantly surpasses the previous best SNN by 9.7% and demonstrates the potential of SNNs for event-based vision. Our model has a concise architecture while maintaining high accuracy and much lower computation cost as a result of sparse computation. Our code will be publicly available.*

## 1. Introduction

Object detection is a fundamental and crucial task in computer vision with a wide range of applications, including face recognition and vehicle and small object detection. Typically, object detection tasks rely on images captured by frame-based cameras. However, images produced by these cameras can be too blurry or slow for high-speed scenarios

or situations with under/overexposure, such as emergency detection during driving. The recently developed retina-inspired Dynamical Vision Sensor (DVS), also known as an event-based sensor [35, 45, 7, 52, 3, 54], solves this problem by recording the intensity changes of pixels at a high temporal resolution of 1 μs with a high dynamical range of 120dB. The sensor generates asynchronous events when the brightness of individual pixels changes, recording the timestamp, polarity, and position of the pixels.

The highly sparse and fluctuating nature of events poses challenges for conventional object detection techniques based on Artificial Neural Networks (ANNs). While recurrent architectural and algorithmic approaches [44, 32] have been proposed for preprocessing events, they often come with high computation costs and increased latency. In contrast, the Spiking Neural Networks (SNNs) are a new type of network inspired by the brain that propagate information through discrete spikes generated from their inherent temporal dynamics. SNNs enable low-cost computation through sparse activation and multiplication-free inference, making them an ideal candidate for processing highly sparse and dynamic events. In addition, SNNs deployed on neuromorphic hardware can also benefit from event-based processing due to the sparse activation.

Recent advancements in surrogate gradient (SG) algorithms [59, 42] have led to the successful training of deep SNNs for image classification tasks [57, 46, 64, 34, 11]. However, the difference between spiking neurons and real-valued artificial neurons in information representation still results in significant performance drops or increased latency when training SNNs for more challenging tasks, such as dense image prediction or object detection [18, 23, 8], especially when their architectures are directly taken from complicated ANNs.

In this work, we study the potential functionalities of various intrinsic temporal dynamics of spiking neurons to explore a low-computation and low-latency approach for processing highly dynamic events. Based on this study, we design an efficient spiking feature pyramid network for event-based object detection, integrating and optimizing these neuronal mechanisms with surrogate gradient training.

\*Corresponding author: lengluziwei@huawei.com, ranchengcn@gmail.com. 1. Department of Computer Science and Engineering, Southern University of Science and Technology, China. 2. ACS Lab, Huawei Technologies, China. 3. Department of Electronic and Electrical Engineering, Southern University of Science and Technology, China.

Our main contributions can be summarized as following:

1. We explore the functionalities of intrinsic temporal dynamics of spiking neurons, including membrane potential dynamics and adaptive threshold, to modulate highly dynamic events and demonstrate that they can strengthen features from sparse events and stabilize training.
2. We design an efficient spiking feature pyramid network for event-based automotive object detection with an optimized spiking encoder architecture.
3. Our proposed SNN outperforms previous SNNs and sophisticated ANNs with attention mechanisms, achieving a mean average precision (map50) of 47.7% on the Gen1 benchmark dataset, significantly surpassing the previous best SNN by 9.7%. Meanwhile, our model has a more concise architecture than ANNs while maintaining high accuracy and much lower computation cost.

## 2. Related Work

### 2.1. Event-based Object Detection

Event cameras, with their high temporal precision and dynamic range, are ideal for scenarios that require high-speed objects, varying lighting conditions, and low latency. However, the dynamic nature of event camera data poses a challenge to traditional deep learning approaches based on frames. To address this challenge, events are usually preprocessed and converted into dense representations before being processed by task networks. There have been several handcrafted methods proposed for this conversion, including event frames [26, 38, 41, 58, 65, 43], stacking based on time or number of events [56], voxel grids [66], the event queue method [55], a grid of LSTMs [5], and discrete time convolution [60]. Special asynchronous convolutions have also been proposed for sparse event data [50, 40]. The latter was applied to the Gen1 event-based automotive object detection dataset [10]. [44] used a convolutional LSTM network and a temporal consistency loss for improved training. ASTMNet [32] proposed an adaptive sampling scheme, with temporal attention and memory modules, to encode events and achieved state-of-the-art accuracy.

### 2.2. Deep SNNs for Vision Tasks

The development of neuromorphic hardware has led to growing interest in using SNNs for hard vision tasks in deep learning [39, 14, 27, 30, 29, 25, 28, 9]. When combined with event cameras, neuromorphic systems can achieve extremely low power and low latency sensing [48]. There are two main approaches for training deep SNNs: ANN-to-SNN conversion and direct training.

The ANN-to-SNN conversion approach approximates real-valued activation functions with spiking mechanisms [49, 51]. Although this approach achieves high accuracy, it also has high latency due to the accumulation of spike rates, making it unsuitable for processing fast events. [23] proposed a spiking version of Yolo for object detection, achieving nearly lossless performance on PASCAL VOC [13] and MS COCO datasets [37] with thousands of timesteps required for convergence. Recent works have reduced latency after conversion [4, 33], but it is unclear whether these methods can be applied to more complex architectures beyond image classification.

The direct training approach uses surrogate gradient (SG) functions to approximate backpropagation gradients [59, 53, 42]. With improved training techniques such as specialized normalization, SG, and loss function design [57, 62, 34, 11], directly trained SNNs are achieving competitive accuracy on hard benchmark classification tasks like ImageNet, with only a few simulation steps required for convergence. These advances have encouraged their application to other event-based vision tasks beyond classification, such as optical flow estimation [18], video reconstruction [67], and object detection [8]. Nevertheless, these works are still limited by relatively simple handcrafted architectures and are suboptimal in terms of accuracy compared to state-of-the-art ANNs. More recently, [6, 61, 31] demonstrated that by using spike-based differentiable hierarchical search, the performance of SNNs can be further improved on multiple event-based vision tasks including challenging deep stereo and semantic segmentation tasks.

## 3. Event Density Modulation with Temporal Dynamics of Spiking Neurons

In automotive scenarios, objects with varying relative speeds captured by event cameras often result in event signals with significant density fluctuations. This poses a challenge for traditional ANNs, which typically deal with images with constant data rates. Spiking neurons, on the other hand, possess abundant temporal dynamics, which are derived from the continuous evolution of their membrane potentials and discrete synaptic transmission processes. In this section, we explore the potential capabilities of two mechanisms, i.e., the dynamics of the membrane potential and the adaptive threshold mechanism, in regulating the radically fluctuating input events.

### 3.1. Event Representation

We adopt the simple stacking based on time (SBT) [56] method for event preprocessing, which is a real-time and low-computation-cost method that is embedded in the accumulator modules of mainstream event sensors. The SBT method combines events into temporally neighboring frames, preserving the rich temporal information of the

event stream that can be potentially learned by the downstream SNN with its inherent temporal dynamics.

Within one stack, the SBT method compresses a duration of  $\Delta t$  event stream into  $n$  frames. The value of each pixel in the  $i$ th frame is defined as the accumulated polarity of events:

$$P(x, y) = \text{sign}(\sum_{t \in T} p(x, y, t)) \quad (1)$$

where  $P$  is the value of the pixel at  $(x, y)$ ,  $t$  is the timestamp,  $p$  is the polarity of the event, and  $T \in [\frac{(i-1)\Delta t}{n}, \frac{i\Delta t}{n}]$  is the duration of events merged into one frame. Another simple event encoding method, stacking based on the number of events (SBN) [56], is compared to SBT in an ablation study. Other more advanced event encoding methods could also be compatible with our network, but may potentially increase computation cost.

### 3.2. Membrane Potential Dynamics

To study the functionality of the membrane potential dynamics of spiking neurons in modulating events, we use the iterative Leaky Integrate and Fire (LIF) model [57] for simplicity. The LIF model is expressed as:

$$\begin{aligned} u_i^{t,n} &= \tau u_i^{t-1,n} (1 - y_i^{t-1,n}) + I_i^{t,n} \\ I_i^{t,n} &= \sum_j w_{ji} y_j^{t,n-1} \end{aligned} \quad (2)$$

with the spike generation formulated as:

$$y_i^{t,n} = H(u_i^{t,n} - u_{\text{th}}) = \begin{cases} 1, & u_i^{t,n} \geq u_{\text{th}} \\ 0, & \text{otherwise} \end{cases} \quad (3)$$

where  $u_i^{t,n}$  represents the membrane potential of the neuron  $i$  of the  $n$ th layer at time  $t$ ,  $\tau$  represents the membrane time constant which configures the membrane leakage of the neuron,  $I_i^{t,n}$  is the influx currency, which is the weighted sum of the spiking activation  $y_j^{t,n-1}$  of the connected neurons from the previous layer  $n-1$ . The spiking activation  $y_i^{t,n}$  is defined by a Heaviside function  $H$  which equals 1 only when  $u_i^{t,n}$  reaches a membrane threshold  $u_{\text{th}}$ , otherwise 0.

When there are too few events during the merging interval, the SBT method may produce a very sparse event frame. Another simple event encoding method, stacking based on the number of events (SBN) [56], solves this problem by using a fixed number of events to form a frame. However, when the event density is too high (e.g. fast moving objects), it can lead to over-blurred frames and suboptimal network performance (see the ablation study in Section 5.3). A recent work [32] proposed an adaptive sampling scheme by iteratively counting an appropriate number of events from temporal bins of adaptive lengths. However, in

practice, this would cause additional computation cost and extra latency.

According to Equation 2, the membrane time constant  $\tau$  controls the proportion of the inherited membrane potential from the previous time step. This accumulation effect of the membrane potential naturally alleviates the sparse events problem, as shown in Figure 1a, where we plot a sample sequence of density of input events alongside with first layer activation using different  $\tau$ . The layer with LIF neurons acts like a low-pass filter when the event density radically fluctuates, modulating its spiking rate at peaks and valleys of event density. Comparatively, the firing rate of the layer with binary neurons (setting  $\tau = 0$ ) is more influenced by the input and exhibits more correlated fluctuations. The modulation effect is also reflected in the network performance, as shown in Table 1. Using a binary neuron leads to a drastic reduction in accuracy, demonstrating the critical role of the temporal dynamics of the membrane potential. In terms of the membrane time constant, we performed experiments with  $\tau$  ranging from 0 to 1 with an interval of 0.1. The performance of the network dropped as  $\tau$  increased further (Figure 1b), indicating that  $\tau$  needs to be in an appropriate range in order for the SNN to have optimal temporal dynamics for the task.

Neuron	Membrane time constant $\tau$	mAP (0.5) %
LIF	0	42.52
LIF	0.1	44.55
LIF	0.2	47.10
LIF	0.3	46.96

Table 1. Results on the Gen1 dataset when applying different membrane time constant.

### 3.3. Adaptive Threshold

In addition to the passive accumulation mechanism of the membrane potential, we investigate a self-adaptive mechanism for the spiking neuron, called the adaptive threshold. Inspired by neuron adaptation in the neocortex [15, 17], the adaptive threshold model has previously been applied to temporal sequence learning in recurrent SNNs [1, 2] to provide long-term memory. Here, we examine its functionality for short-term modulation of events. The adaptive threshold is formulated as:

$$\begin{aligned} y^t &= H(u^t - A^t) \\ A^t &= u_{\text{th}} + \beta a^t \\ a^t &= \tau_a a^{t-1} + y^{t-1} \end{aligned} \quad (4)$$

where  $H$  is the Heaviside step function,  $A^t$  is the adjustable threshold at time  $t$ ,  $a^t$  is the cumulative threshold increment that changes according to the spiking history of the neuron,  $\beta$  is a scaling factor, and  $\tau_a$  is the time constant of  $a$ . The

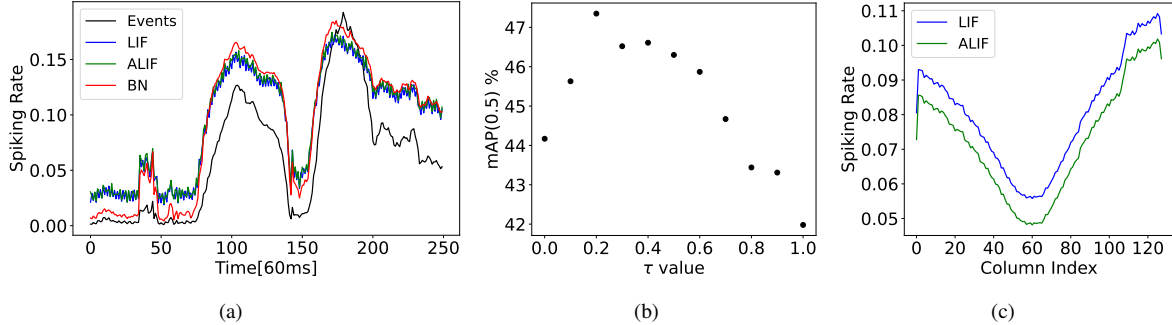


Figure 1. (a) A sample sequence of event density and the first layer activation using the LIF ( $\tau = 0.2$ ), ALIF ( $\tau = 0.2$ ) and binary neuron (BN). Each data point on the 'Events' curve is an averaged event density of an SBT stack with 60ms duration. The layer activation is calculated by averaging the spiking feature map. (b) Mean precision with different  $\tau$  values for LIF neuron, results were averaged over 3 experiments with different random seeds. (c) Averaged column firing rate of the first layer over the test set. Average column spiking rate of the first layer on the test set for LIF and ALIF neurons, results were averaged over 4 experiments with different random seeds. The mean and variance of mAP(0.5) for LIF and ALIF neurons are  $46.62 \pm 0.29$  and  $47.38 \pm 0.34$ , respectively. The "V" shape profile is due to relatively less events from far objects.

adjustable threshold  $A$  modulates the spiking rate such that the threshold rises during dense input, which suppresses the neuron from firing, and vice versa. The upper and lower bounds of the adaptive threshold can be derived by considering extreme input scenarios. When the neuron is continuously inactive,  $a^t \rightarrow 0$  as  $t \rightarrow \infty$ , meaning the lower bound of  $A^t$  is the original threshold  $u_{\text{th}}$ . In the extreme case when the neuron is continuously active, with  $y^0 = 1$  and  $a^0 = 0$ ,  $a^t$  can be expressed as

$$a^t = \sum_{i=1}^t \tau_a^{i-1} \quad (5)$$

and its upper bound can be derived as  $t \rightarrow \infty$  and equals  $1/(1 - \tau_a)$ . The range of the adjustable threshold  $A$  is therefore  $[u_{\text{th}}, u_{\text{th}} + \beta/(1 - \tau_a)]$ . This event-triggered, self-adaptive activity improves the network's robustness and stability to rapidly fluctuating event densities, and could further improve the performance of the SNN.

To verify our hypothesis, we compare the performance of a network using LIF neurons with a network using LIF neurons with adaptive threshold (ALIF). We conduct experiments where we use ALIF neurons for the whole network, as well as only for the first layer of the network (with the rest of the network using LIF neurons). During the experiments, we set  $\tau_a$  as a trainable variable with each layer sharing the same value. The results are summarized in Table 2.

For multiple random seeds, the network with ALIF neurons applied to the first layer outperforms both networks with LIF neurons, with  $u_{\text{th}}$  set to 0.3 and 0.4, which correspond to the lower and upper bounds of the adaptive threshold (refer to section 5.1 for details). This demonstrates the effectiveness of the adaptive threshold in processing dynamic events. However, applying ALIF neurons to the

whole network results in suboptimal performance. We believe that an excessive use of adjustable thresholds might lead to excessive network flexibility and harm training precision. In terms of firing rate, ALIF neuron leads to higher layer sparsity as shown in Figure 1c, demonstrating the advantage of self-adaptive thresholds for events encoding.

Neuron	Layer	Threshold	mAP (0.5) %
LIF	All/First	0.3	$47.0 \pm 0.1$
LIF	First	0.4	47.0
ALIF	All	0.3	40.0
ALIF	First	0.3	<b><math>47.6 \pm 0.2</math></b>

Table 2. Results on the Gen1 dataset when applying different neuron model on the first and all layers of the network.

### 3.4. Surrogate Gradient Training

The challenge of training an SNN lies in the discontinuity of spike generation, as no gradient can be applied for backpropagation. The early success of deep SNNs in machine learning tasks was achieved by transferring ANN-trained model parameters to their equivalent SNN [12, 49]. Using rate coding, the activation of an analog neuron is proportional to the firing rate of its corresponding spiking neuron in the converted SNN. However, this approach is usually restricted to feed-forward network architectures without recurrence and is therefore only applicable to tasks with weak temporal dependencies.

On the other hand, surrogate gradient methods approximate the discontinuous activation by smoothing out the spike generation function (such as Equation 3), allowing for the calculation of gradients for backpropagation. During training, the temporal neural dynamics are precisely modeled (Equation 2) and the errors can be backpropagated

through time. As a result, surrogate gradient methods not only enable training of spiking neurons considering precise temporal dynamics, but are also naturally suited to solving tasks with temporal dependencies such as the continuous object detection in this paper.

We adopt the Dspike surrogate function proposed by [34]:

$$\text{Dspike}(u) = a \cdot \tanh(b(u - c)) + d, 0 \leq u \leq 1$$

$$\tanh(x) = \frac{e^x - e^{-x}}{e^x + e^{-x}}, \quad (6)$$

where  $u$  is the membrane potential and parameters  $(a, b, c, d)$  transform the original hyperbolic tangent function  $\tanh$  to output in the range  $[0, 1]$  with different shapes. The wide range of surrogate function choices satisfies various training requirements. Particularly,  $b$ , the so-called temperature factor, controls the smoothness of the surrogate function.  $c$  is usually set to 0.5 to set a symmetry center at  $u = 0.5$ , and parameters  $c$  and  $d$  are tuned to ensure  $\text{Dspike}(0) = 0$  and  $\text{Dspike}(1) = 1$ . Other SG functions could also be used for the training.

## 4. Spiking Feature Pyramid Network

Despite recent progress in SNNs for image classification [57, 46, 64, 34, 11], there are still few examples of SNNs demonstrating competitive precision with ANNs in more challenging vision tasks, such as object detection. Directly applying sophisticated ANN architectures to SNNs often leads to suboptimal performance or extra latency, especially when the task requires efficient structural variation of the network [18, 23, 8]. While there have been ongoing efforts to improve ANN-to-SNN conversion methods [4, 33], we take a different approach by designing an efficient network specifically for spiking neurons, which we present in this section.

### 4.1. Encoder Backbone

The encoder network typically takes up the largest portion of parameters in a detector and its feature extraction capability is critical to the network's performance. ResNet [20] and its derivatives are commonly used as backbones in detection networks. In the field of SNNs, spiking ResNets [51, 34, 11] are currently the norm for image classification. Recently, an alternative architecture was proposed by [6] that achieves higher accuracy in deep SNNs by organizing spiking activities as hierarchical directed acyclic graphs (HDAGs). We design the encoder backbone following this principle and compare spiking HDAG with spiking ResNet as encoder under similar model capacities in our ablation study.

As shown in Figure 2, the encoder backbone follows a multi-stage downsampling architecture, consisting of two

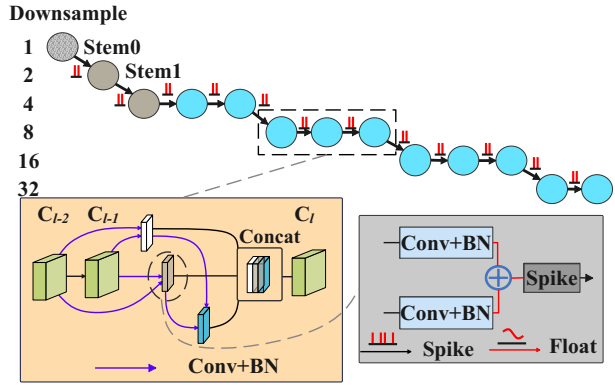


Figure 2. Encoder Backbone. The backbone follows a multi-stage downsampling architecture consisting of multiple cells connected as directed acyclic graphs. Two spiking convolution layers (denoted as stem layers) are used for initial channel variation. The cell connection topology is repeated across different layers. Within the cell, operations on the node are summed up on the membrane potential level and finally go through a spiking function.

spiking stem layers followed by ten spiking cells. During downsampling, the spatial resolution of the feature map is halved while the channel size is doubled. A spiking stem layer consists of a convolution, batch normalization (which can be later merged into convolution weights during test inference [22]), and a spiking activation function. These layers are used for initial feature extraction and channel variation. The spiking cell contains three spiking nodes, and its structure is repeated across layers. The first two nodes receive inputs from two previous cells and the third node receives input from the previous two nodes. The feature maps of all nodes share the same size, and their outputs are concatenated to form the output of the cell. Within each node, operations from multiple edges are summed up on the membrane potential level and then passed through a spiking activation function. The connection of the spiking cell is designed empirically to strike a balance between inference speed and accuracy. Other potential connection topologies can be explored in the future. A detailed architecture of the backbone is provided in the supplement.

### 4.2. Network Architecture

Feature pyramids have been widely used in many object detection systems to provide multi-scale feature information [19, 36, 63]. In our approach, we integrate the output spiking feature maps from the last three stages of the backbone to form a spiking feature pyramid, as shown in Figure 3. The features with lower spatial resolution in the pyramid are upsampled by nearest interpolation to double the width and height (to maintain a binary feature map) and concatenated with feature maps of the same spatial dimension from the backbone. These features are then fused

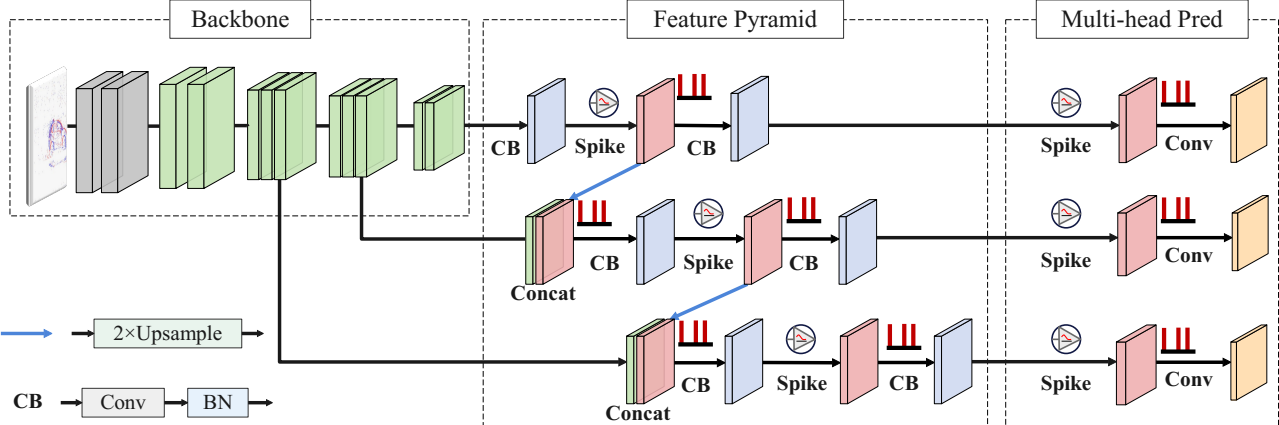


Figure 3. Overall network architecture. The spiking feature pyramid network consists of a encoder backbone implemented by a multi-stage spiking network. The spiking feature pyramid is integrated from output feature maps at different stage of the backbone. A multi-head prediction module takes the output of the feature pyramid through parallel spiking convolution layers and generates multiple prediction boxes which are finally selected by the NMS method. The network follows full spike-based computation and performs multiplication-free inference.

through a  $1 \times 1$  convolution, batch normalization, and spike activation to form the next level of the feature pyramid. The spiking feature pyramid is fed to a multi-head prediction module through convolution, batch normalization, and spike activation. The resulting features are processed by a  $1 \times 1$  convolution to produce floating-point results of shape  $N \times N \times [3 \times (C + 5)]$ , where  $N$  represents the width and height of the corresponding feature map,  $C$  is the number of categories, and 5 corresponds to 4 box coordinate predictions and 1 confidence prediction. We use non-maximum suppression (NMS) [47, 16] to select the final bounding boxes.

## 5. Experiment

We conduct experiments on the widely used Gen1 [10] dataset, a large scale event-based automotive object detection dataset which contains more than 39 hours of automotive recordings acquired with a Prophesee GEN1 ATIS sensor (resolution  $304 \times 240$ ), together with more than 255,000 manual bounding box annotations of cars and pedestrians. These bounding boxes are labeled at 1Hz, 2Hz or 4Hz. All data is split into training, validation and test sets where recordings are cut into 60 seconds chunks with each set containing 1460, 429 and 470 videos.

### 5.1. Implementation Details

#### Input Representation

The events generated by the sensor in real-world scenarios are consecutive and have variable lengths. To fully utilize the temporal information of event data, we use  $S \times C$  frames ahead of the label timestamp as input for each sample during training. Here,  $S$  is the number of SBT stacks and  $C$  is

the number of frames in each stack. As per Equation 1, we set  $\Delta t = 60\text{ms}$ ,  $n = C = 3$ , and  $S = 3$ . This results in a minimum temporal resolution of  $T = \frac{\Delta t}{n} = 20\text{ms}$  with a frame-based update scheme.

The output of the network at the last stack is used for prediction. This way, the temporal information can be accumulated and learned by the system for the task.

#### Hyperparameters

During the training phase, we use the Adamw optimizer with an initial learning rate of  $1e^{-3}$  and a weight decay of  $5e^{-4}$ . No pre-training is required, all models are directly trained for 30 epochs with a batch size of 32 and use a warm up policy with the learning rate of the first epoch gradually increases from a very low value to the initial learning rate. The LIF and ALIF neurons have a membrane time constant  $\tau$  of 0.2 and a membrane threshold  $u_{th}$  of 0.3. The temperature  $b$  of the  $D\text{spike}$  function is set to 3. For the ALIF neuron, we use  $\beta = 0.07$  and  $\tau_a$  is set to a learnable parameter with initial value of 0.3 and limited to  $[0.2, 0.4]$ . For event-based object detection, we use COCO mAP [37] as the metric for accuracy and report both mAP(0.5) and mAP(0.5:0.95). The overlap threshold is set to 0.5 and the predicting score is set to 0.3.

### 5.2. Results

We compare our methods with previous works of both SNNs and ANNs, the results are reported in Table 3, values of other models are taken from literature. In SNN domain, our network significantly surpasses 3 models in [8] by 9.7-12.7 % on mAP(0.5) and 3.4-7.6 % on mAP(0.5:0.95) meanwhile with fewer time steps for convergence. Our network also slightly surpasses ASTMNet [32], a recently proposed ANN with attention mechanism and handcrafted

Model	Type	Params	(T)	mAP(0.5)	mAP(0.5:0.95)
SparseConv [40]	ANN	133M	-	15.0	-
Events-RetinaNet [44]	ANN	33M	-	34.0	-
E2Vid-RetinaNet [44]	ANN	44M	-	27.0	-
RED [44]	ANN	24M	-	40.0	-
Gray-RetinaNet [44]	ANN	33M	-	44.0	-
ASTMNet [32]	ANN	-	-	46.7	-
VGG-11+SDD [8]	SNN	13M	5	37	17.4
MobileNet-64+SSD [8]	SNN	24M	5	35	14.7
DenseNet121-24+SSD [8]	SNN	8M	5	38	18.9
<b>FP-DAGNet (Ours)</b>	SNN	<b>22M</b>	<b>3</b>	<b>47.7</b>	<b>22.3</b>

Table 3. Result on Gen1 dataset. - denotes data not available.

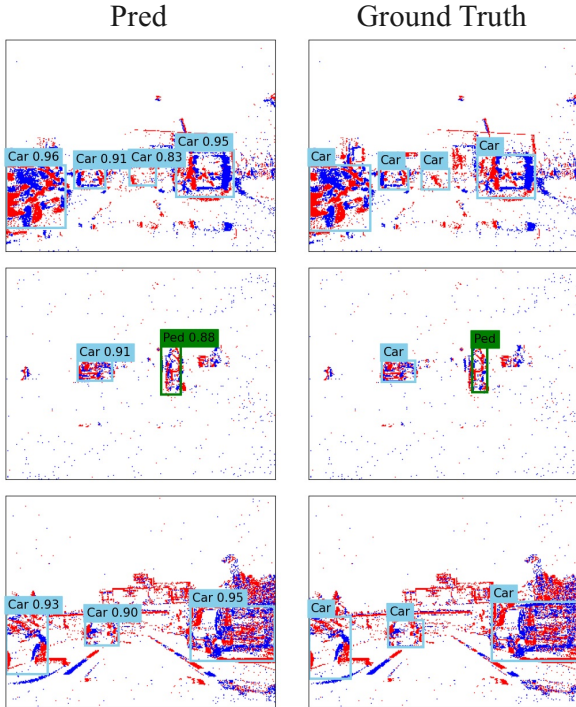


Figure 4. Prediction results of our model and the corresponding ground truth. Ped stands for pedestrian.

adaptive sampling event preprocessing schemes, meanwhile with much concise architecture. These results demonstrate the effectiveness of our model and the potential of SNN in processing highly sparse and dynamic events. A few samples from the prediction results of our model are shown in Figure 4.

In real-world scenario, events are generated consecutively by the sensor with flexible lengths. To test the real-time applicability of our model, we feed the entire test split continuously into the model, which evolves an equal length of steps and estimates sequential labels. The average inference speed of one stack reaches 54 FPS (Tesla V100 GPU).

### 5.3. Ablation Study

Method	S	C	mAP(0.5)	mAP(0.5:0.95)
SBN+LIF	2	5	43.56	19.70
SBN+LIF	3	3	43.24	19.44
SBT+LIF	2	5	47.58	22.24
SBT+LIF	3	3	47.10	21.76
SBT+ALIF	2	5	47.31	21.91
SBT+ALIF	3	3	<b>47.70</b>	<b>22.27</b>

Table 4. Results with different input configurations. S represents the number of stacks, C represents the number of frames in a stack.

#### Input Configuration

To investigate the impact of different preprocessing methods and input configurations, we compare the results using SBN and SBT with LIF neurons. For both methods, we apply two sets of input configurations with different numbers of stacks and frames: S=3, C=3 and S=2, C=5. For SBT, each frame contains events within 20 ms, whereas for SBN, each frame contains 5000 events. In addition, we apply the ALIF neuron (to the first layer) for SBT to compare the influence of neuron type at different input configurations. The results are shown in Table 4. For the LIF neuron, the overall accuracy of using SBN is lower than that of SBT, and using both SBN and SBT for S=3, C=3 is worse than S=2, C=5. The result of using SBT with ALIF neurons is opposite, with the best result obtained at S=3, C=3. The results demonstrate that SBT is better than SBN, and that the ALIF neuron performs better in the SBT approach with a larger number of stacks, where the neuron has longer time to adapt its threshold.

#### Adaptive Threshold

We further perform experiments to investigate the hyperparameter sensitivity of adaptive threshold and the effectiveness of training  $\tau_a$ . The results are summarized in Table 5. The model demonstrates robust performance in a range of different values of  $\beta$ . In addition, network with a trainable  $\tau_a$  performs better than with a fixed value.

#### Spiking ResNet

Initial $\tau_a$	$\beta$	mAP(0.5) %	mAP(0.5:0.95) %
0.3	0.05	47.3	21.7
0.3	0.07	47.7	22.3
0.3 (fixed)	0.07	47.0	21.9
0.3	0.09	47.1	22.0

Table 5. Results with different hyperparameter setting of the adaptive threshold.  $\tau_a$  (fixed) denotes that the variable is not trainable and fixed to a certain value.

To study the contribution of our specific encoder backbone design on network performance, we implement the backbone with an alternative architecture, i.e. spiking ResNet, which is widely used in image classification. We choose spiking ResNet-18 since it is also a 4-stage downsample structure. For a fair comparison, we select a range of channel sizes for the network covering a range of model capacities. The results are summarized in Table 6. Under similar model size, ResNet with initial channel size 80 performs worse than DAGNet. We conjecture that the large number of inter and intra-cell connections within the DAGNet benefits information flow and gradient propagation in the training of the deep SNN. More details of the architecture of the ResNet are provided in the supplement.

Architecture	ICS	Model size	mAP (0.5)	mAP (0.5:0.95)
ResNet18	64	13.34M	41.63	17.99
ResNet18	80	20.82M	42.08	18.96
ResNet18	96	29.97M	44.29	19.92
<b>DAGNet</b>	<b>48</b>	<b>21.63M</b>	<b>47.70</b>	<b>22.27</b>

Table 6. Results on Gen1 dataset with different backbone architectures. ICS stands for initial channel size.

#### 5.4. Network Sparsity and Computation Cost

In this section, we compare the computation cost of our methods with previous works of ANN and SNN. Due to spike-based sparse computation and multiplication-free inference, SNNs can achieve significant computation drop compare to ANNs base on dense matrix multiplication. As Figure 5 shows, our network exhibits an overall sparse activity with varying degrees across layers. The average network sparsity and computation cost are summarized in Table 7. The spiking FP-DAGNet has much higher sparsity and lower operation number compares with previous SNNs. Following [34, 46, 24], we count the number of addition operations of the SNN by  $s * T * A$ , where  $s$  is the mean sparsity,  $T$  is the time step and  $A$  is the addition number. The energy consumption is estimated following the study of [21] on 45nm CMOS technology adopted by previous works [34, 46, 6], with one addition operation in SNN costing 0.9pJ while one multiply-accumulate (MAC) operation in

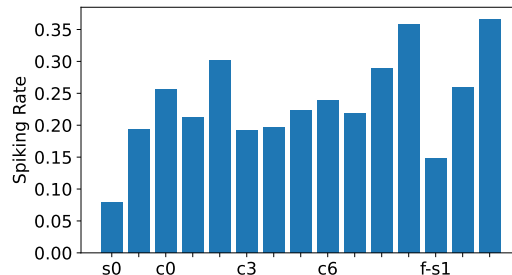


Figure 5. Network sparsity of spiking FP-DAGNet. The network exhibits an overall sparse activity with varying degrees across layers, with the highest sparsity at the first layer due to highly sparse input event streams.

Model	# OP.	Sparsity	Energy (mJ)
Events-RetinaNet (ANN)	18.73G	-	86.16
VGG-11+SDD	12.30G	22.22%	11.07
MobileNet-64+SSD	6.39G	29.44%	5.74
DenseNet121-24+SSD	4.33G	37.20%	3.90
<b>FP-DAGNet</b>	<b>2.83G</b>	<b>19.10%</b>	<b>2.55</b>

Table 7. Comparison of operation number (OP) and estimated energy cost. For SNN number of addition operations is counted and for ANN number of multiplication-addition operations is counted.

ANN consuming 4.6pJ. For ANN we use Events-RetinaNet [44] since there is a lack of detailed architecture descriptions or publicly available code for other works. Compare to Events-RetinaNet, our SNN achieves more than 6 times less operation number and more than 33 times less of estimated energy consumption, demonstrating the great potential of SNNs for low-power event-based vision.

#### 6. Conclusion

In this work, we explore the functionalities of membrane potential dynamics and adaptive threshold of spiking neurons in processing highly sparse and dynamic events. The event feature strengthening and network training stabilization abilities demonstrated by these mechanisms are also of general usage for other event-based vision tasks. Based on these neuronal mechanisms, we develop an efficient spiking feature pyramid network with an optimized spiking encoder backbone. On the large-scale event-based automotive object detection dataset of Gen1, our SNN significantly outperforms the previous best SNN and also surpasses sophisticated ANNs with attention mechanism, meanwhile with more concise architectures and much lower computation cost, demonstrating the potential of SNN for event-based vision. A potential implementation of our model on neuromorphic hardware can further accelerate its inference speed, creating neuromorphic systems realizing extremely

low power and low latency sensing.

## References

- [1] Guillaume Bellec, Darjan Salaj, Anand Subramoney, Robert Legenstein, and Wolfgang Maass. Long short-term memory and learning-to-learn in networks of spiking neurons. *Advances in neural information processing systems*, 31, 2018. 3
- [2] Guillaume Bellec, Franz Scherr, Anand Subramoney, Elias Hajek, Darjan Salaj, Robert Legenstein, and Wolfgang Maass. A solution to the learning dilemma for recurrent networks of spiking neurons. *Nature communications*, 11(1):3625, 2020. 3
- [3] Christian Brandli, Raphael Berner, Minhao Yang, Shih-Chii Liu, and Tobi Delbrück. A  $240 \times 180$  130 db  $3 \mu\text{s}$  latency global shutter spatiotemporal vision sensor. *IEEE Journal of Solid-State Circuits*, 49(10):2333–2341, 2014. 1
- [4] Tong Bu, Wei Fang, Jianhao Ding, PengLin Dai, Zhaofei Yu, and Tiejun Huang. Optimal ann-snn conversion for high-accuracy and ultra-low-latency spiking neural networks. In *International Conference on Learning Representations*, 2021. 2, 5
- [5] Marco Cannici, Marco Ciccone, Andrea Romanoni, and Matteo Matteucci. A differentiable recurrent surface for asynchronous event-based data. In *European Conference on Computer Vision*, pages 136–152. Springer, 2020. 2
- [6] Kaiwei Che, Liziwei Leng, Kaixuan Zhang, Jianguo Zhang, Qinghu Meng, Jie Cheng, Qinghai Guo, and Jianxing Liao. Differentiable hierarchical and surrogate gradient search for spiking neural networks. *Advances in Neural Information Processing Systems*, 35:24975–24990, 2022. 2, 5, 8
- [7] Shoushun Chen, Wei Tang, Xiangyu Zhang, and Eugenio Culurciello. A  $64 \times 64$  pixels uwb wireless temporal-difference digital image sensor. *IEEE transactions on very large scale integration (VLSI) systems*, 20(12):2232–2240, 2011. 1
- [8] Loïc Cordone, Benoît Miramond, and Philippe Thierion. Object detection with spiking neural networks on automotive event data, 2022. 1, 2, 5, 6, 7
- [9] Mike Davies, Andreas Wild, Garrick Orchard, Yulia Sandamirskaya, Gabriel A Fonseca Guerra, Prasad Joshi, Philipp Plank, and Sumedh R Risbud. Advancing neuromorphic computing with loihi: A survey of results and outlook. *Proceedings of the IEEE*, 109(5):911–934, 2021. 2
- [10] Pierre de Tournemire, Davide Nitti, Etienne Perot, Davide Migliore, and Amos Sironi. A large scale event-based detection dataset for automotive, 2020. 2, 6
- [11] Shikuang Deng, Yuhang Li, Shanghang Zhang, and Shi Gu. Temporal efficient training of spiking neural network via gradient re-weighting. *arXiv preprint arXiv:2202.11946*, 2022. 1, 2, 5
- [12] Peter U Diehl, Daniel Neil, Jonathan Binas, Matthew Cook, Shih-Chii Liu, and Michael Pfeiffer. Fast-classifying, high-accuracy spiking deep networks through weight and threshold balancing. In *2015 International joint conference on neural networks (IJCNN)*, pages 1–8. ieee, 2015. 4
- [13] Mark Everingham, Luc Van Gool, Christopher KI Williams, John Winn, and Andrew Zisserman. The pascal visual object classes (voc) challenge. *International journal of computer vision*, 88(2):303–338, 2010. 2
- [14] Steve B Furber, Francesco Galluppi, Steve Temple, and Luis A Plana. The spinnaker project. *Proceedings of the IEEE*, 102(5):652–665, 2014. 2
- [15] Wulfram Gerstner, Werner M Kistler, Richard Naud, and Liam Paninski. *Neuronal dynamics: From single neurons to networks and models of cognition*. Cambridge University Press, 2014. 3
- [16] Ross Girshick, Jeff Donahue, Trevor Darrell, and Jitendra Malik. Rich feature hierarchies for accurate object detection and semantic segmentation. In *Proceedings of the IEEE conference on computer vision and pattern recognition*, pages 580–587, 2014. 6
- [17] Nathan W Gouwens, Jim Berg, David Feng, Staci A Sorensen, Hongkui Zeng, Michael J Hawrylycz, Christof Koch, and Anton Arkhipov. Systematic generation of biophysically detailed models for diverse cortical neuron types. *Nature communications*, 9(1):710, 2018. 3
- [18] Jesse Hagaars, Federico Paredes-Vallés, and Guido De Croon. Self-supervised learning of event-based optical flow with spiking neural networks. *Advances in Neural Information Processing Systems*, 34, 2021. 1, 2, 5
- [19] Kaiming He, Xiangyu Zhang, Shaoqing Ren, and Jian Sun. Spatial pyramid pooling in deep convolutional networks for visual recognition. *IEEE transactions on pattern analysis and machine intelligence*, 37(9):1904–1916, 2015. 5
- [20] Kaiming He, Xiangyu Zhang, Shaoqing Ren, and Jian Sun. Deep residual learning for image recognition. In *Proceedings of the IEEE conference on computer vision and pattern recognition*, pages 770–778, 2016. 5
- [21] Mark Horowitz. 1.1 computing’s energy problem (and what we can do about it). In *2014 IEEE International Solid-State Circuits Conference Digest of Technical Papers (ISSCC)*, pages 10–14. IEEE, 2014. 8
- [22] Sergey Ioffe and Christian Szegedy. Batch normalization: Accelerating deep network training by reducing internal covariate shift. In *International Conference on Machine Learning*, pages 448–456. PMLR, 2015. 5
- [23] Seijo Kim, Seongsik Park, Byunggoon Na, and Sungroh Yoon. Spiking-yolo: spiking neural network for energy-efficient object detection. In *Proceedings of the AAAI Conference on Artificial Intelligence*, volume 34, pages 11270–11277, 2020. 1, 2, 5
- [24] Youngeun Kim, Joshua Chough, and Priyadarshini Panda. Beyond classification: Directly training spiking neural networks for semantic segmentation. *arXiv preprint arXiv:2110.07742*, 2021. 8
- [25] Akos F Kungl, Sebastian Schmitt, Johann Klähn, Paul Müller, Andreas Baumbach, Dominik Dold, Alexander Kugele, Eric Müller, Christoph Koke, Mitja Kleider, et al. Accelerated physical emulation of bayesian inference in spiking neural networks. *Frontiers in neuroscience*, page 1201, 2019. 2
- [26] Xavier Lagorce, Garrick Orchard, Francesco Galluppi, Bertram E Shi, and Ryad B Benosman. Hots: a hierarchy

of event-based time-surfaces for pattern recognition. *IEEE transactions on pattern analysis and machine intelligence*, 39(7):1346–1359, 2016. 2

[27] Liziwei Leng. *Deep learning architectures for neuromorphic hardware*. PhD thesis, Master thesis, Ruprecht-Karls-Universität Heidelberg, 2014. HD-KIP 14-26, 2014. 2

[28] Liziwei Leng. *Solving Machine Learning Problems with Biological Principles*. PhD thesis, 2020. 2

[29] Liziwei Leng, Roman Martel, Oliver Breitwieser, Ilja Bytschok, Walter Senn, Johannes Schemmel, Karlheinz Meier, and Mihai A Petrovici. Spiking neurons with short-term synaptic plasticity form superior generative networks. *Scientific reports*, 8(1):1–11, 2018. 2

[30] Liziwei Leng, Mihai A Petrovici, Roman Martel, Ilja Bytschok, Oliver Breitwieser, Johannes Bill, Johannes Schemmel, and Karlheinz Meier. Spiking neural networks as superior generative and discriminative models. *Cosyne Abstracts, Salt Lake City USA*, 2016. 2

[31] Boyan Li, Liziwei Leng, Ran Cheng, Shuaijie Shen, Kaixuan Zhang, Jianguo Zhang, and Jianxing Liao. Efficient deep spiking multi-layer perceptrons with multiplication-free inference. *arXiv preprint arXiv:2306.12465*, 2023. 2

[32] Jianing Li, Jia Li, Lin Zhu, Xijie Xiang, Tiejun Huang, and Yonghong Tian. Asynchronous spatio-temporal memory network for continuous event-based object detection. *IEEE Transactions on Image Processing*, 31:2975–2987, 2022. 1, 2, 3, 6, 7

[33] Yuhang Li, Shikuang Deng, Xin Dong, Ruihao Gong, and Shi Gu. A free lunch from ann: Towards efficient, accurate spiking neural networks calibration. In *International Conference on Machine Learning*, pages 6316–6325. PMLR, 2021. 2, 5

[34] Yuhang Li, Yufei Guo, Shanghang Zhang, Shikuang Deng, Yongqing Hai, and Shi Gu. Differentiable spike: Rethinking gradient-descent for training spiking neural networks. *Advances in Neural Information Processing Systems*, 34:23426–23439, 2021. 1, 2, 5, 8

[35] Patrick Lichtsteiner, Christoph Posch, and Tobi Delbrück. A  $128 \times 128$  120 db  $15\mu\text{s}$  latency asynchronous temporal contrast vision sensor. *IEEE journal of solid-state circuits*, 43(2):566–576, 2008. 1

[36] Tsung-Yi Lin, Piotr Dollar, Ross Girshick, Kaiming He, Bharath Hariharan, and Serge Belongie. Feature pyramid networks for object detection. In *Proceedings of the IEEE Conference on Computer Vision and Pattern Recognition (CVPR)*, July 2017. 5

[37] Tsung-Yi Lin, Michael Maire, Serge Belongie, James Hays, Pietro Perona, Deva Ramanan, Piotr Dollár, and C Lawrence Zitnick. Microsoft coco: Common objects in context. In *European conference on computer vision*, pages 740–755. Springer, 2014. 2, 6

[38] Ana I Maqueda, Antonio Loquercio, Guillermo Gallego, Narciso García, and Davide Scaramuzza. Event-based vision meets deep learning on steering prediction for self-driving cars. In *Proceedings of the IEEE Conference on Computer Vision and Pattern Recognition*, pages 5419–5427, 2018. 2

[39] Paul A Merolla, John V Arthur, Rodrigo Alvarez-Icaza, Andrew S Cassidy, Jun Sawada, Filipp Akopyan, Bryan L Jackson, Nabil Imam, Chen Guo, Yutaka Nakamura, et al. A million spiking-neuron integrated circuit with a scalable communication network and interface. *Science*, 345(6197):668–673, 2014. 2

[40] Nico Messikommer, Daniel Gehrig, Antonio Loquercio, and Davide Scaramuzza. Event-based asynchronous sparse convolutional networks. In *European Conference on Computer Vision*, pages 415–431. Springer, 2020. 2, 7

[41] Diederik Paul Moeys, Federico Corradi, Emmett Kerr, Philip Vance, Gautham Das, Daniel Neil, Dermot Kerr, and Tobi Delbrück. Steering a predator robot using a mixed frame/event-driven convolutional neural network. In *2016 Second International Conference on Event-based Control, Communication, and Signal Processing (EBCCSP)*, pages 1–8. IEEE, 2016. 2

[42] Emre O Neftci, Hesham Mostafa, and Friedemann Zenke. Surrogate gradient learning in spiking neural networks: Bringing the power of gradient-based optimization to spiking neural networks. *IEEE Signal Processing Magazine*, 36(6):51–63, 2019. 1, 2

[43] Anh Nguyen, Thanh-Toan Do, Darwin G Caldwell, and Nikos G Tsagarakis. Real-time 6dof pose relocalization for event cameras with stacked spatial lstm networks. In *Proceedings of the IEEE/CVF Conference on Computer Vision and Pattern Recognition Workshops*, pages 0–0, 2019. 2

[44] Etienne Perot, Pierre de Tournemire, Davide Nitti, Jonathan Masci, and Amos Sironi. Learning to detect objects with a 1 megapixel event camera. *Advances in Neural Information Processing Systems*, 33:16639–16652, 2020. 1, 2, 7, 8

[45] Christoph Posch, Daniel Matolin, and Rainer Wohlgemant. A qvga 143 db dynamic range frame-free pwm image sensor with lossless pixel-level video compression and time-domain cds. *IEEE Journal of Solid-State Circuits*, 46(1):259–275, 2010. 1

[46] Nitin Rathi and Kaushik Roy. Diet-snn: A low-latency spiking neural network with direct input encoding and leakage and threshold optimization. *IEEE Transactions on Neural Networks and Learning Systems*, 2021. 1, 5, 8

[47] Joseph Redmon and Ali Farhadi. Yolo9000: better, faster, stronger. In *Proceedings of the IEEE conference on computer vision and pattern recognition*, pages 7263–7271, 2017. 6

[48] Kaushik Roy, Akhilesh Jaiswal, and Priyadarshini Panda. Towards spike-based machine intelligence with neuromorphic computing. *Nature*, 575(7784):607–617, 2019. 2

[49] Bodo Rueckauer, Iulia-Alexandra Lungu, Yuhuang Hu, Michael Pfeiffer, and Shih-Chii Liu. Conversion of Continuous-Valued Deep Networks to Efficient Event-Driven Networks for Image Classification. *Frontiers in Neuroscience*, 11:682, 2017. 2, 4

[50] Cedric Scheerlinck, Nick Barnes, and Robert Mahony. Asynchronous spatial image convolutions for event cameras. *IEEE Robotics and Automation Letters*, 4(2):816–822, 2019. 2

[51] Abhranil Sengupta, Yuting Ye, Robert Wang, Chiao Liu, and Kaushik Roy. Going deeper in spiking neural networks: Vgg

and residual architectures. *Frontiers in neuroscience*, 13:95, 2019. [2](#), [5](#)

[52] Teresa Serrano-Gotarredona and Bernabé Linares-Barranco. A  $128 \times 128$  1.5% contrast sensitivity 0.9% fpn  $3 \mu\text{s}$  latency 4 mw asynchronous frame-free dynamic vision sensor using transimpedance preamplifiers. *IEEE Journal of Solid-State Circuits*, 48(3):827–838, 2013. [1](#)

[53] Sumit B Shrestha and Garrick Orchard. Slayer: Spike layer error reassignment in time. *Advances in neural information processing systems*, 31, 2018. [2](#)

[54] Bongki Son, Yunjae Suh, Sungho Kim, Heejae Jung, Jun-Seok Kim, Changwoo Shin, Keunju Park, Kyoojin Lee, Jin-man Park, Jooyeon Woo, et al. 4.1 a  $640 \times 480$  dynamic vision sensor with a  $9\mu\text{m}$  pixel and 300meps address-event representation. In *2017 IEEE International Solid-State Circuits Conference (ISSCC)*, pages 66–67. IEEE, 2017. [1](#)

[55] Stepan Tulyakov, Francois Fleuret, Martin Kiefel, Peter Gehler, and Michael Hirsch. Learning an event sequence embedding for dense event-based deep stereo. In *Proceedings of the IEEE/CVF International Conference on Computer Vision*, pages 1527–1537, 2019. [2](#)

[56] Lin Wang, Yo-Sung Ho, Kuk-Jin Yoon, et al. Event-based high dynamic range image and very high frame rate video generation using conditional generative adversarial networks. In *Proceedings of the IEEE/CVF Conference on Computer Vision and Pattern Recognition*, pages 10081–10090, 2019. [2](#), [3](#)

[57] Yujie Wu, Lei Deng, Guoqi Li, Jun Zhu, Yuan Xie, and Luting Shi. Direct training for spiking neural networks: Faster, larger, better. In *Proceedings of the AAAI Conference on Artificial Intelligence*, volume 33, pages 1311–1318, 2019. [1](#), [2](#), [3](#), [5](#)

[58] C Ye, A Mitrokhin, C Parameshwara, C Fermüller, JA Yorke, and Y Aloimonos. Unsupervised learning of dense optical flow and depth from sparse event data. *corr abs/1809.08625* (2018), 1809. [2](#)

[59] Friedemann Zenke and Surya Ganguli. Superspike: Supervised learning in multilayer spiking neural networks. *Neural computation*, 30(6):1514–1541, 2018. [1](#), [2](#)

[60] Kaixuan Zhang, Kaiwei Che, Jianguo Zhang, Jie Cheng, Ziyang Zhang, Qinghai Guo, and Liziwei Leng. Discrete time convolution for fast event-based stereo. In *Proceedings of the IEEE/CVF Conference on Computer Vision and Pattern Recognition*, pages 8676–8686, 2022. [2](#)

[61] Rui Zhang, Liziwei Leng, Kaiwei Che, Hu Zhang, Jie Cheng, Qinghai Guo, Jiangxing Liao, and Ran Cheng. Accurate and efficient event-based semantic segmentation using adaptive spiking encoder-decoder network. *arXiv preprint arXiv:2304.11857*, 2023. [2](#)

[62] Wenrui Zhang and Peng Li. Temporal spike sequence learning via backpropagation for deep spiking neural networks. *Advances in Neural Information Processing Systems*, 33:12022–12033, 2020. [2](#)

[63] Zhong-Qiu Zhao, Peng Zheng, Shou-Tao Xu, and Xindong Wu. Object detection with deep learning: A review. *IEEE Transactions on Neural Networks and Learning Systems*, 30(11):3212–3232, 2019. [5](#)

[64] Hanle Zheng, Yujie Wu, Lei Deng, Yifan Hu, and Guoqi Li. Going deeper with directly-trained larger spiking neural networks. In *Proceedings of the AAAI Conference on Artificial Intelligence*, volume 35, pages 11062–11070, 2021. [1](#), [5](#)

[65] Alex Zihao Zhu, Liangzhe Yuan, Kenneth Chaney, and Kostas Daniilidis. Ev-flownet: Self-supervised optical flow estimation for event-based cameras. *arXiv preprint arXiv:1802.06898*, 2018. [2](#)

[66] Alex Zihao Zhu, Liangzhe Yuan, Kenneth Chaney, and Kostas Daniilidis. Unsupervised event-based learning of optical flow, depth, and egomotion. In *Proceedings of the IEEE/CVF Conference on Computer Vision and Pattern Recognition*, pages 989–997, 2019. [2](#)

[67] Lin Zhu, Xiao Wang, Yi Chang, Jianing Li, Tiejun Huang, and Yonghong Tian. Event-based video reconstruction via potential-assisted spiking neural network. *arXiv preprint arXiv:2201.10943*, 2022. [2](#)